Next-to-next-to-leading order evolution of polarized parton densities in the Larin scheme

J. Blümlein[1,2] and M. Saragnese[1,3]

[1]*Deutsches Elektronen-Synchrotron DESY, Platanenallee 6, 15738 Zeuthen, Germany*
[2]*Institut für Theoretische Physik III, IV, TU Dortmund, Otto-Hahn Straße 4, 44227 Dortmund, Germany*
[3]*Wolfram Research, Inc., 100 Trade Center Drive Champaign, IL 61820-7237, USA*

(Received 28 May 2024; accepted 24 June 2024; published 6 August 2024)

In many calculations involving polarized twist-2 parton densities to higher order in the strong coupling constant one uses the Larin scheme to describe chiral effects in dimensional regularization. Upon forming observables, the scheme dependence cancels. Still one needs a corresponding regularization scheme to compute the contributing building blocks, like massless and massive Wilson coefficients, as well as the massive three-loop operator matrix elements used in the variable flavor number scheme. These are matched to the evolved parton distribution functions in the Larin scheme. Starting with suitable input distributions we provide the solution of scale evolution of the different polarized parton distribution functions in Bjorken x space for a wide range of virtualities Q^2 in the Larin scheme, at next-to-leading, at next-to-next-to-leading order for the first time. We also illustrate the deviation between the parton distributions in the Larin and $\overline{\rm MS}$ schemes numerically.

DOI: 10.1103/PhysRevD.110.034006

I. INTRODUCTION

In the calculation of the scaling violations of polarized hadronic processes the building blocks of the factorized processes are scheme dependent. Working in dimensional regularization one may either use the Larin scheme [1] or the HVBM scheme [2–7] to describe the Dirac matrix γ_5 in $D = 4 + \varepsilon$ dimensions. Computing the Lorentz- and Dirac-structures of the corresponding scattering processes by using `Form` [8], reference to the Larin scheme is particularly efficient. Finally, one forms observables, such as the structure functions of deep-inelastic scattering [9–14], or other hard-scattering processes. The initial scheme dependence of the Wilson coefficients and parton distribution functions (PDFs) cancels in the observables.[1]

For this reason, we provide the solution of the polarized partonic evolution equations in the Larin scheme at next-to-leading order (NLO) and next-to-next-to-leading order (NNLO) in the present paper, following earlier representations at NLO in the $\overline{\rm MS}$ scheme [17]. At leading order (LO) the evolution of parton distributions is scheme invariant. To perform a consistent expansion of the corresponding evolution equations algebraically we work in Mellin–N space, cf. Ref. [18]. The results are presented in terms of grids in the virtuality Q^2 and the Bjorken variable x for $4\ \text{GeV}^2 \le Q^2 \le 10^6\ \text{GeV}^2$ and $10^{-9} \le x < 1$.[2] The shapes of the PDFs are parametrized at $Q_0^2 = 4\ \text{GeV}^2$, fixing $\alpha_s^{\rm NLO}(M_Z^2) = 0.1191$ from the fit [19] and $\alpha_s^{\rm NNLO}(M_Z^2) = 0.1147$ from the analysis in Ref. [20]. Here the strong coupling constant is defined by $\alpha_s = g_{s,\rm ren}^2/(4\pi) \equiv a_s(4\pi)$. In the leading order evolution we use the starting value $\alpha_s^{\rm NLO}(Q_0^2)$, because leading order QCD fits are unstable. This leads to $\alpha_s^{\rm LO}(M_Z^2) = 0.1247$. The values of $\alpha_s(M_Z^2)$ determined in the polarized data analysis [17] are consistent with these values, although the current errors are much larger than for the values obtained using unpolarized deep-inelastic scattering data due to the current statistics of the polarized World data.

The polarized anomalous dimensions at LO were calculated in [21–23], at NLO in [24–26] and NNLO in Refs. [27–31]. The massless Wilson coefficients at $O(a_s)$ were computed in [32–36], at $O(a_s^2)$ in [37,38] and at $O(a_s^3)$ in the nonsinglet case in [39,40] and the singlet case in Ref. [40]. Finally, the massive Wilson coefficients at LO were obtained in [41]. Numerical results at NLO were computed in [42]. In the asymptotic region $Q^2 \gg m_Q^2$ the massive Wilson coefficients and massive operator matrix elements (OMEs) were calculated at NLO in [43–46], even

[1]Alternatively, one may consider scheme-invariant evolution of structure functions, see Refs. [15,16] and references therein.

[2]Lower values of Q^2 lay outside the deep-inelastic region and require the separation of resonant and (quasi)elastic contributions.

Published by the American Physical Society under the terms of the Creative Commons Attribution 4.0 International license. Further distribution of this work must maintain attribution to the author(s) and the published article's title, journal citation, and DOI. Funded by SCOAP³.

before [42], and at NNLO in Refs. [47–54] in the single mass case. The corresponding three-loop two-mass corrections were calculated in Refs. [55–57]. For all quantities up to $O(a_s^2)$ the transformation from the Larin to the $\overline{\rm MS}$ scheme is known. The polarized asymptotic heavy flavor contributions of $O(a_s^3)$, i.e. the NNLO corrections, depend also on the three-loop massless Wilson coefficients and are given in the Larin scheme. This also applies to the transition coefficients in the variable flavor number scheme at $O(a_s^3)$. In these cases the PDFs in the Larin scheme have to be used in representing the scaling violations of the corresponding observables. It finally turns out that the deviations of the evolution of different parton densities are larger than the projected accuracy for future polarized deep-inelastic scattering experiments of $O(1\%)$ [58].

The paper is organized as follows. In Sec. II we describe the parametrization of the polarized parton densities and details of the evolution. Some numerical comparisons of the results in the $\overline{\rm MS}$ and Larin schemes are given in Secs. III and IV contains the conclusions. The parametrizations in the $\overline{\rm MS}$ and Larin schemes are provided in ancillary files [59] in form of grids and a numerical program which allows for spline interpolation in the kinematic regions to be considered.

II. THE PARAMETRIZATION AND DETAILS OF THE EVOLUTION

The PDFs of the polarized quarks and antiquarks $\Delta q_i(x,Q^2)$, as well as of the polarized gluon density $\Delta G(x,Q^2)$, are parametrized at the scale $Q_0^2 = 4$ GeV^2, cf. [17],[3] by

$$x\Delta f_i(x,Q_0^2) = \eta_i A_i x^{a_i}(1-x)^{b_i}(1+\gamma_i x), \quad f = q, G \tag{1}$$

with the normalization constants A_i, being given by

$$A_i^{-1} = \left(1 + \gamma_i \frac{a_i}{a_i + b_i + 1}\right) B(a_i, b_i + 1). \tag{2}$$

The parameters η_i denote the first moments

$$\eta_i = \int_0^1 dx \Delta f_i(x,Q_0^2) \tag{3}$$

of the respective distributions. The values of the initial parameters are given in Table 2 of Ref. [17]. Here η_{u_v} and η_{d_v} are fixed by the F and D parameters measured in neutron and hyperon β–decays. $B(a,b) = \Gamma(a)\Gamma(b)/\Gamma(a+b)$ denotes Euler's B-function, related to Euler's Γ-function.

In the case of three massless flavors the following two flavor nonsinglet distributions contribute

$$\Delta_3^{\rm NS,-} = (\Delta u + \Delta\bar{u}) - (\Delta d + \Delta\bar{d}), \tag{4}$$

$$\Delta_8^{\rm NS,-} = (\Delta u + \Delta\bar{u}) + (\Delta d + \Delta\bar{d}) - 2(\Delta s + \Delta\bar{s}). \tag{5}$$

Furthermore, there is the nonsinglet distribution $\Delta q^{\rm NS,v}$,

$$\Delta q^{\rm NS,v} = \sum_{i=1}^{3} [\Delta q_i - \Delta\bar{q}_i]. \tag{6}$$

The distributions $\Delta_{3(8)}^{\rm NS,-}$ evolve with the splitting function $\Delta P^{\rm NS,-} = P^{\rm NS,+}$ and $q^{\rm NS,v}$ with $\Delta P^{\rm NS,-} + \Delta P^{\rm NS,s}$. The splitting function $\Delta P^{\rm NS,s}$ is computable at even values of N and is continued to $N \in \mathbb{C}$.[4] $\Delta P^{\rm NS,s}$ [31,70] is scheme independent at three-loop order and $P^{\rm NS,+}$ derives from a vector current. Therefore, to three-loop order, there is no impact of the Larin scheme on this quantity. The distribution (6) can be measured from the interference structure function $g_5^-(x,Q^2)$, see Ref. [71]. For a completely symmetric polarized sea, $\Delta u_s = \Delta d_s = \Delta\bar{u} = \Delta\bar{d} = \Delta s = \Delta\bar{s}$, which we will consider, the relation

$$\Delta q^{\rm NS,v}(x) = \Delta_8^{\rm NS,-}(x) \tag{7}$$

holds at the input scale Q_0^2.

The polarized singlet distribution is given by

$$\Delta\Sigma = \sum_{i=1}^{3} [\Delta q_i + \Delta\bar{q}_i], \tag{8}$$

which evolves together with the polarized gluon distribution ΔG. The differences in the anomalous dimensions between the Larin and the $\overline{\rm MS}$ scheme start at NLO. They are implied by the correction terms $z_{qq}^{(k),\rm NS}$ and $z_{qq}^{(k+1),\rm PS}$, $k \geq 1$, cf. [28,31,72].

The evolution equations in the polarized case consist of three flavor nonsinglet evolution equations to NNLO [27,30] and the coupled singlet and gluon distribution evolution [28,31]. In the latter case one solves matrix-valued differential equations. In Mellin–N space the corresponding iterative solutions can be obtained analytically. Here one expands systematically in $a_s(\mu^2)$, with $\mu^2 = Q^2$ and $\mu^2 = Q_0^2$ up to a given order l with $O(a_s^{l-m}(Q^2) a_s^m(Q_0^2)), m \in \{0,\ldots,l\}$, see Ref. [18], Sec. 5.1, for details. The solution in x-space is obtained by a single contour integral around the singularities of the problem, see

[3]Here it has been shown that this parametrization is close to those obtained in other analyses, see, e.g. [60–67] and Figures 2 and 3, [17], for comparisons at the initial scale Q_0^2.

[4]Our evolution program is written such that all quantities are free of factors $(-1)^N$. This can be obtained as outlined in Refs. [68,69].

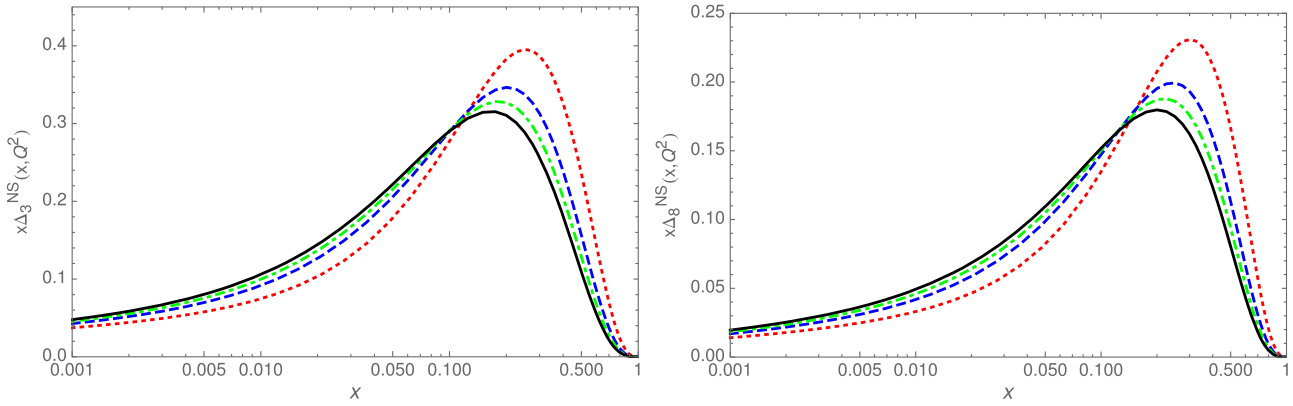

FIG. 1. The evolution of the polarized nonsinglet densities $x\Delta_3^{\mathrm{NS},-}$ and $x\Delta_8^{\mathrm{NS},-}$ in the $\overline{\mathrm{MS}}$ scheme at NNLO. Dotted lines: $Q^2 = 4$ GeV^2, dashed lines: $Q^2 = 100$ GeV^2, dash-dotted lines: $Q^2 = 1000$ GeV^2, full lines: $Q^2 = 10000$ GeV^2.

Refs. [73,74]. This representation avoids pile-up contributions for the parton distributions by iterative solutions of the evolution equation, which were discussed in Ref. [75]. They have, otherwise, to be removed by using the method described in [76,77], see also [78].[5] The evolution of the strong coupling constant $a_s(Q^2)$ is calculated numerically in the respective regions of constant N_F, cf., e.g. [79], performing the matching at $Q^2 = m_c^2$, m_b^2, and m_t^2 by using the on-shell masses [80,81],

$$m_c = 1.59\,\mathrm{GeV}, \quad m_b = 4.78\,\mathrm{GeV}, \quad m_t = 172.5\,\mathrm{GeV}, \tag{9}$$

according to [82]. The expansion coefficients of the β-function were calculated in Refs. [83–94].

III. NUMERICAL RESULTS

In the following we consider the evolution of the nonsinglet distributions (4)–(6) and of the polarized singlet and gluon distribution. Depending on whether the structure function $g_1(x, Q^2)$ is measured at a proton or deuteron target (after nuclear corrections), cf. [16], both the distributions (4), (5) or only (5) contribute, while (6) appears only for polarized structure functions with an axialvector–vector contribution, as e.g. for $g_5^-(x, Q^2)$. To three-loop order the choice of the scheme has, however, no effect on the evolution of this distribution. For this reason we do not consider this case here.

The grid files are named `PolLO(NLO,NNLO)M(L)` for the PDFs contributing to $g_1(x, Q^2)$, respectively. Here, the files at LO are the same in the Larin (L) and $\overline{\mathrm{MS}}$ (M) scheme. We use a cubic spline interpolation[6] both in x and Q^2 in the parametrized kinematic region, see Sec. I. The attached `FORTRAN` code `Npolpdf.f` provides the values of the respective distributions.

We first illustrate the evolution of the $x\Delta_3^{\mathrm{NS},-}$, $x\Delta_8^{\mathrm{NS},-}$, $x\Delta\Sigma$ and $x\Delta G$, as functions in x and Q^2 in the $\overline{\mathrm{MS}}$ scheme in Figs. 1–2 at NNLO. While the maximum of the distributions deplete in the quarkonic case with growing values of Q^2, they rise for the gluon. In the gluonic case the maxima shift more strongly to lower values of x, compared to the quarkonic cases. The evolution leads to a growth of the distributions in the range of smaller values of x, while they are depleted in the large x region for rising values of the virtuality Q^2. The singlet distribution is negative in the region of smaller values of x due to the negative sea quark distributions.

We now compare the deviations of the different distributions considered in the Larin (L) and $\overline{\mathrm{MS}}$ scheme (M),

$$r(x, Q^2) = \frac{f^{\mathrm{L}}(x, Q^2)}{f^{\mathrm{M}}(x, Q^2)} - 1 \tag{10}$$

at NNLO for the values of $Q^2 = 100$, 1000 and 10000 GeV^2 as functions of x. In Fig. 3 we illustrate the deviation for the nonsinglet distributions $x\Delta_3^{\mathrm{NS},-}$ and $x\Delta_8^{\mathrm{NS},-}$. The deviations are similar for both distributions and grow towards small value of x.

In Figs. 4 and 5 we show the deviation for the singlet distributions $x\Delta\Sigma$ and $x\Delta G$. While the effect is larger for $x\Delta\Sigma$ due to the change in the quarkonic splitting functions, the one for $x\Delta G$ is relatively small, since the splitting functions $\Delta P_{gg}^{(k)}$ are not affected and the changes come only from convolutions with other splitting functions. The large relative effects in the range of medium values of x in the ratio for $x\Delta\Sigma$ are due to zero transitions for this quantity. Similar results are obtained at NLO.

All ratios $r(x, Q^2)$ turn to zero for $x \to 1$. This is due to the fact that the difference of splitting functions $\Delta P_{qq}^{+,(1),\mathrm{NS}}$,

[5]One may even expand whole observables in $a_s(Q^2)$ and $a_s(Q_0^2)$ to obtain completely scheme-invariant quantities, see Ref. [16].

[6]We thank S. Kumano and M. Miyama of AAC Collaboration for allowing us to use their interpolation routines.

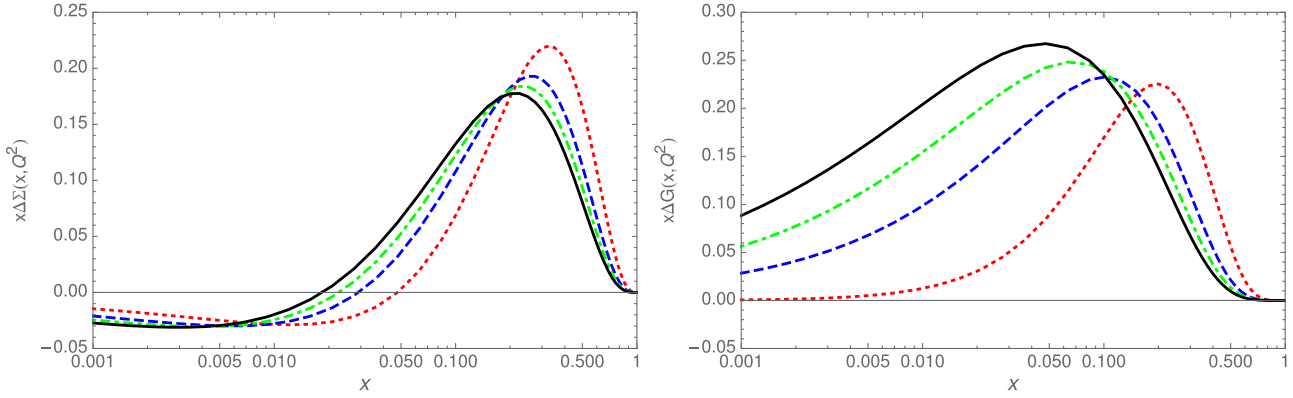

FIG. 2. The evolution of the polarized singlet and gluon densities $x\Delta\Sigma$ and $x\Delta G$ in the $\overline{\rm MS}$ scheme at NNLO. Dotted lines: $Q^2 = 4$ GeV^2, dashed lines: $Q^2 = 100$ GeV^2, dash-dotted lines: $Q^2 = 1000$ GeV^2, full lines: $Q^2 = 10000$ GeV^2.

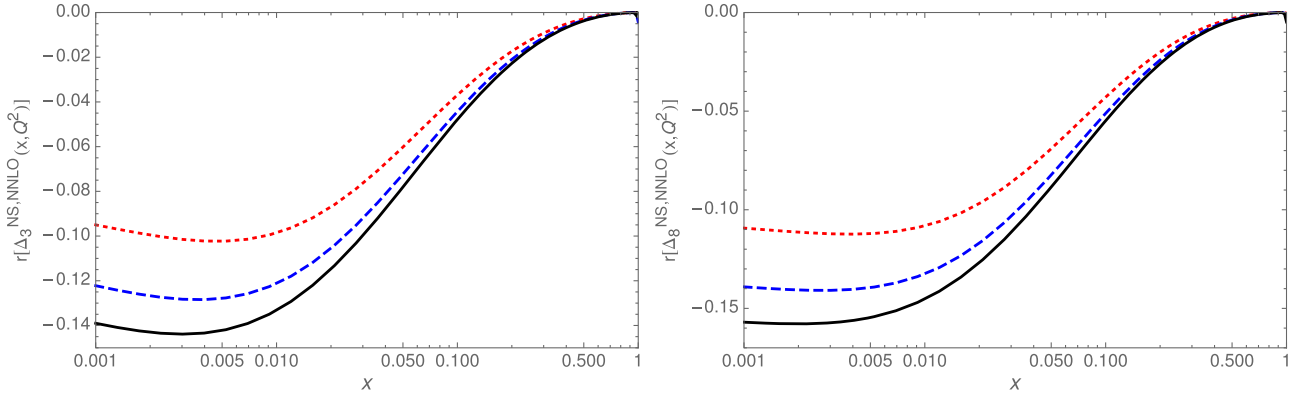

FIG. 3. The function $r(x, Q^2)$, Eq. (10), for the evolution at NNLO; dotted lines: $Q^2 = 100$ GeV^2, dashed lines: $Q^2 = 1000$ GeV^2, full lines: $Q^2 = 10000$ GeV^2. Left panel: $\Delta_3^{\rm NS,-}$. Right panel: $\Delta_8^{\rm NS,-}$.

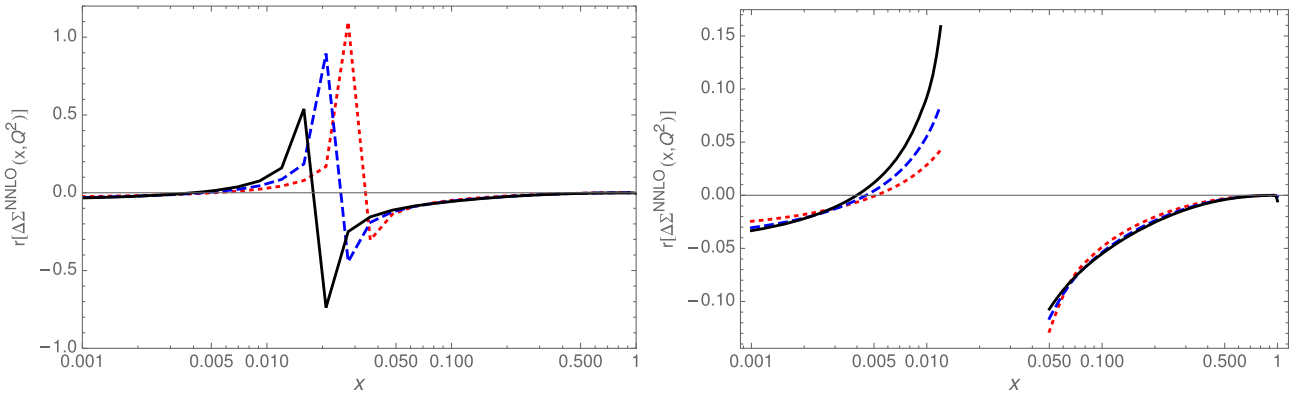

FIG. 4. The function $r(x, Q^2)$, Eq. (10), for the evolution at NNLO; dotted lines: $Q^2 = 100$ GeV^2, dashed lines: $Q^2 = 1000$ GeV^2, full lines: $Q^2 = 10000$ GeV^2. Left panel: $\Delta\Sigma$. Right panel: $\Delta\Sigma$, enlarging the small and large x regions and excluding the zero-transition region.

$\Delta P_{qg}^{(1)}$ and $\Delta P_{gq}^{(1)}$ are $\propto 1/N^3$ and $\Delta P_{qq}^{+,(2),\rm NS} \propto \ln(N)/N^3$, $\Delta P_{qq}^{(2),\rm PS} \propto 1/N^3$ and $\Delta P_{qg}^{(2)}, \Delta P_{gq}^{(2)} \propto \ln^2(N)/N^3$, where the large N behavior rules that at large values of x. From Figs. 3 and 4 one sees that the evolution of the polarized parton densities are different in the $\overline{\rm MS}$ and the Larin schemes, although at different degree. They have to be taken into account in precision analyses.

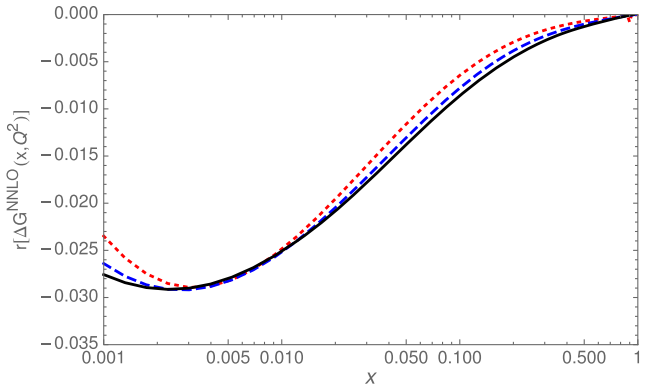

FIG. 5. The function $r(x, Q^2)$, Eq. (10), for the evolution of ΔG at NNLO; dotted lines: $Q^2 = 100$ GeV^2, dashed lines: $Q^2 = 1000$ GeV^2, full lines: $Q^2 = 10000$ GeV^2.

IV. CONCLUSIONS

We have calculated the evolution of polarized parton distribution functions in the Larin scheme in a wide range of the kinematic variables x and Q^2 at NLO and NNLO. These distributions can be used to form observables in cases in which polarized Wilson coefficients, hard-scattering subsystem cross sections or massive operator matrix elements were calculated in this scheme only. This allows for a consistent data analysis. It is already clear from the results on the nonsinglet distributions leading to corrections of up to $O(15\%)$ in the small x range, $x \gtrsim 0.001$, that the polarized parton distributions in both schemes are significantly different, given, e.g. the future experimental accuracies to be reached at the EIC [58,95]. One therefore needs the PDFs in the Larin scheme, to describe the flavor matching in the variable flavor number scheme and for incorporating the heavy flavor Wilson coefficients in the polarized case into data analysis of deep-inelastic structure functions and hard-scattering cross sections at polarized hadron colliders.

For comparison, we also performed the corresponding evolution in the $\overline{\rm MS}$ scheme at LO, NLO and NNLO. We provide both sets of grids and the corresponding `FORTRAN` program in an ancillary file to this paper [59].

ACKNOWLEDGMENTS

We would like to thank A. Behring, P. Marquard, E. Reya and K. Schönwald for discussions.

[1] S. A. Larin, The renormalization of the axial anomaly in dimensional regularization, Phys. Lett. B **303**, 113 (1993).
[2] G. 't Hooft and M. J. G. Veltman, Regularization and renormalization of gauge fields, Nucl. Phys. **B44**, 189 (1972).
[3] D. A. Akyeampong and R. Delbourgo, Dimensional regularization, abnormal amplitudes and anomalies, Nuovo Cimento Soc. Ital. Fis. **17A**, 578 (1973).
[4] D. A. Akyeampong and R. Delbourgo, Dimensional regularization and PCAC, Nuovo Cimento Soc. Ital. Fis. A **18**, 94 (1973).
[5] D. A. Akyeampong and R. Delbourgo, Anomalies via dimensional regularization, Nuovo Cimento Soc. Ital. Fis. **19A**, 219 (1974).
[6] P. Breitenlohner and D. Maison, Dimensionally renormalized Green's functions for theories with massless particles. 1., Commun. Math. Phys. **52**, 39 (1977).
[7] P. Breitenlohner and D. Maison, Dimensionally renormalized Green's functions for theories with massless particles. 2., Commun. Math. Phys. **52**, 55 (1977).
[8] J. A. M. Vermaseren, New features of FORM, arXiv:math-ph/0010025.
[9] H. D. Politzer, Asymptotic freedom: An approach to strong interactions, Phys. Rep. **14**, 129 (1974).
[10] B. Geyer, D. Robaschik, and E. Wieczorek, Theory of deep inelastic lepton-hadron scattering. 1., Fortschr. Phys. **27**, 75 (1979).
[11] A. J. Buras, Asymptotic freedom in deep inelastic processes in the leading order and beyond, Rev. Mod. Phys. **52**, 199 (1980).
[12] E. Reya, Perturbative quantum chromodynamics, Phys. Rep. **69**, 195 (1981).
[13] B. Lampe and E. Reya, Spin physics and polarized structure functions, Phys. Rep. **332**, 1 (2000).
[14] J. Blümlein, The theory of deeply inelastic scattering, Prog. Part. Nucl. Phys. **69**, 28 (2013).
[15] J. Blümlein and A. Guffanti, Scheme-invariant NNLO evolution for unpolarized DIS structure functions, Nucl. Phys. B, Proc. Suppl. **152**, 87 (2006).
[16] J. Blümlein and M. Saragnese, The N^{3}LO scheme-invariant QCD evolution of the non-singlet structure functions $F_2^{\rm NS}(x, Q^2)$ and $g_1^{\rm NS}(x, Q^2)$, Phys. Lett. B **820**, 136589 (2021).
[17] J. Blümlein and H. Böttcher, QCD analysis of polarized deep inelastic scattering data, Nucl. Phys. **B841**, 205 (2010).
[18] J. Blümlein and A. Vogt, The evolution of unpolarized singlet structure functions at small x, Phys. Rev. D **58**, 014020 (1998).
[19] S. Alekhin, J. Blümlein, and S. Moch, NLO PDFs from the ABMP16 fit, Eur. Phys. J. C **78**, 477 (2018).
[20] S. Alekhin, J. Blümlein, S. Moch, and R. Placakyte, Parton distribution functions, α_s, and heavy-quark masses for LHC Run II, Phys. Rev. D **96**, 014011 (2017).
[21] K. Sasaki, Polarized electroproduction in asymptotically free gauge theories, Prog. Theor. Phys. **54**, 1816 (1975).

[22] M. A. Ahmed and G. G. Ross, Spin-dependent deep inelastic electron scattering in an asymptotically free gauge theory, Phys. Lett. **56B**, 385 (1975).
[23] G. Altarelli and G. Parisi, Asymptotic freedom in parton language, Nucl. Phys. **B126**, 298 (1977).
[24] R. Mertig and W. L. van Neerven, The calculation of the two loop spin splitting functions $P_{ij}^{(1)}(x)$, Z. Phys. C **70**, 637 (1996).
[25] W. Vogelsang, A rederivation of the spin dependent next-to-leading order splitting functions, Phys. Rev. D **54**, 2023 (1996).
[26] W. Vogelsang, The spin dependent two loop splitting functions, Nucl. Phys. **B475**, 47 (1996).
[27] S. Moch, J. A. M. Vermaseren, and A. Vogt, The three loop splitting functions in QCD: The nonsinglet case, Nucl. Phys. **B688**, 101 (2004).
[28] S. Moch, J. A. M. Vermaseren, and A. Vogt, The three-loop splitting functions in QCD: The helicity-dependent case, Nucl. Phys. **B889**, 351 (2014).
[29] A. Behring, J. Blümlein, A. De Freitas, A. Goedicke, S. Klein, A. von Manteuffel, C. Schneider, and K. Schönwald, The polarized three-loop anomalous dimensions from on-shell massive operator matrix elements, Nucl. Phys. **B948**, 114753 (2019).
[30] J. Blümlein, P. Marquard, C. Schneider, and K. Schönwald, The three-loop unpolarized and polarized non-singlet anomalous dimensions from off shell operator matrixelements, Nucl. Phys. **B971**, 115542 (2021).
[31] J. Blümlein, P. Marquard, C. Schneider, and K. Schönwald, The three-loop polarized singlet anomalous dimensions from off-shell operator matrix elements, J. High Energy Phys. 01 (2022) 193.
[32] W. Furmanski and R. Petronzio, Lepton—hadron processes beyond leading order in quantum chromodynamics, Z. Phys. C **11**, 293 (1982).
[33] J. Kodaira, S. Matsuda, T. Muta, K. Sasaki, and T. Uematsu, QCD effects in polarized electroproduction, Phys. Rev. D **20**, 627 (1979).
[34] J. Kodaira, S. Matsuda, K. Sasaki, and T. Uematsu, QCD higher order effects in spin dependent deep inelastic electroproduction, Nucl. Phys. **B159**, 99 (1979).
[35] I. Antoniadis and C. Kounnas, Factorization properties and their probabilistic interpretation in polarized electroproduction and annihilation processes, Phys. Rev. D **24**, 505 (1981).
[36] G. T. Bodwin and J. W. Qiu, The gluonic contribution to G (1) and its relationship to the spin dependent parton distributions, Phys. Rev. D **41**, 2755 (1990).
[37] E. B. Zijlstra and W. L. van Neerven, $O(\alpha_s^2)$ corrections to the polarized structure function $g_1(x, Q^2)$, Nucl. Phys. **B417**, 61 (1994); **B426**, 245(E) (1994); **B773**, 105 (2007); **B501**, 599 (1997).
[38] A. Vogt, S. Moch, M. Rogal, and J. A. M. Vermaseren, Towards the NNLO evolution of polarised parton distributions, Nucl. Phys. B, Proc. Suppl. **183**, 155 (2008).
[39] J. A. M. Vermaseren, A. Vogt, and S. Moch, The third-order QCD corrections to deep-inelastic scattering by photon exchange, Nucl. Phys. **B724**, 3 (2005).
[40] J. Blümlein, P. Marquard, C. Schneider, and K. Schönwald, The massless three-loop Wilson coefficients for the deep-inelastic structure functions F_2, F_L, xF_3 and g_1, J. High Energy Phys. 11 (**2022**) 156.
[41] A. D. Watson, Spin spin asymmetries in inclusive muon proton charm production, Z. Phys. C **12**, 123 (1982).
[42] F. Hekhorn and M. Stratmann, Next-to-leading order QCD corrections to inclusive heavy-flavor production in polarized deep-inelastic scattering, Phys. Rev. D **98**, 014018 (2018).
[43] M. Buza, Y. Matiounine, J. Smith, and W. L. van Neerven, $O(\alpha_s^2)$ corrections to polarized heavy flavor production at $Q^2 \gg m^2$, Nucl. Phys. **B485**, 420 (1997).
[44] I. Bierenbaum, J. Blümlein, and S. Klein, Two-loop massive operator matrix elements for polarized and unpolarized deep-inelastic scattering, *Proceedings of the DIS 2007*, edited by G. Grindhammer and K. Sachs (2007), pp. 821–824 [Report No. DESY-PROC-2007-01], 10.3204/proc07-01/148.
[45] J. Blümlein, C. Raab, and K. Schönwald, The polarized two-loop massive pure singlet Wilson coefficient for deep-inelastic scattering, Nucl. Phys. **B948**, 114736 (2019).
[46] I. Bierenbaum, J. Blümlein, A. De Freitas, A. Goedicke, S. Klein, and K. Schönwald, $O(\alpha_s^2)$ polarized heavy flavor corrections to deep-inelastic scattering at $Q^2 \gg m^2$, Nucl. Phys. **B988**, 116114 (2023).
[47] J. Ablinger, A. Behring, J. Blümlein, A. De Freitas, A. Hasselhuhn, A. von Manteuffel, M. Round, C. Schneider, and F. Wißbrock, The 3-loop non-singlet heavy flavor contributions and anomalous dimensions for the structure function $F_2(x, Q^2)$ and transversity, Nucl. Phys. **B886**, 733 (2014).
[48] A. Behring, J. Blümlein, A. De Freitas, A. von Manteuffel, and C. Schneider, The 3-loop non-singlet heavy flavor contributions to the structure function $g_1(x, Q^2)$ at large momentum transfer, Nucl. Phys. **B897**, 612 (2015).
[49] J. Ablinger, A. Behring, J. Blümlein, A. De Freitas, A. von Manteuffel, C. Schneider, and K. Schönwald, The three-loop single mass polarized pure singlet operator matrix element, Nucl. Phys. **B953**, 114945 (2020).
[50] A. Behring, J. Blümlein, A. De Freitas, A. von Manteuffel, K. Schönwald, and C. Schneider, The polarized transition matrix element $A_{gq}(N)$ of the variable flavor number scheme at $O(\alpha_s^3)$, Nucl. Phys. **B964**, 115331 (2021).
[51] J. Blümlein, A. De Freitas, M. Saragnese, C. Schneider, and K. Schönwald, Logarithmic contributions to the polarized $O(\alpha_s^3)$ asymptotic massive Wilson coefficients and operator matrix elements in deeply inelastic scattering, Phys. Rev. D **104**, 034030 (2021).
[52] J. Ablinger, A. Behring, J. Blümlein, A. De Freitas, A. Goedicke, A. von Manteuffel, C. Schneider, and K. Schönwald, The unpolarized and polarized single-mass three-loop heavy flavor operator matrix elements $A_{gg,Q}$ and $\Delta A_{gg,Q}$, J. High Energy Phys. 12 (2022) 134.
[53] J. Ablinger, A. Behring, J. Blümlein, A. De Freitas, A. von Manteuffel, C. Schneider, and K. Schönwald, The first–order factorizable contributions to the three–loop massive operator matrix elements $A_{Qg}^{(3)}$ and $\Delta A_{Qg}^{(3)}$, Nucl. Phys. **B999**, 116427 (2024).

[54] J. Ablinger, A. Behring, J. Blümlein, A. De Freitas, A. von Manteuffel, C. Schneider, and K. Schönwald, The non-first-order-factorizable contributions to the three-loop single-mass operator matrix elements $A_{Qg}^{(3)}$ and $\Delta A_{Qg}^{(3)}$ Phys. Lett. B **854**, 138713 (2024).

[55] J. Ablinger, J. Blümlein, A. De Freitas, A. Hasselhuhn, C. Schneider, and F. Wißbrock, Three loop massive operator matrix elements and asymptotic Wilson coefficients with two different masses, Nucl. Phys. **B921**, 585 (2017).

[56] J. Ablinger, J. Blümlein, A. De Freitas, M. Saragnese, C. Schneider, and K. Schönwald, The three-loop polarized pure singlet operator matrix element with two different masses, Nucl. Phys. **B952**, 114916 (2020).

[57] J. Ablinger, J. Blümlein, A. De Freitas, A. Goedicke, M. Saragnese, C. Schneider, and K. Schönwald, The two-mass contribution to the three-loop polarized gluonic operator matrix element $A_{gg,Q}^{(3)}$, Nucl. Phys. **B955**, 115059 (2020).

[58] R. Abdul Khalek, A. Accardi, J. Adam, D. Adamiak, W. Akers, M. Albaladejo, A. Al-bataineh, M. G. Alexeev, F. Ameli, P. Antonioli *et al.*, Science requirements and detector concepts for the electron-ion collider: EIC yellow report, Nucl. Phys. **A1026**, 122447 (2022).

[59] See Supplemental Material at http://link.aps.org/supplemental/10.1103/PhysRevD.110.034006 for the README-file describes the ancillary files to this paper.

[60] Y. Goto *et al.* (Asymmetry Analysis Collaboration), Polarized parton distribution functions in the nucleon, Phys. Rev. D **62**, 034017 (2000).

[61] M. Hirai, S. Kumano, and N. Saito (Asymmetry Analysis Collaboration), Determination of polarized parton distribution functions and their uncertainties, Phys. Rev. D **69**, 054021 (2004).

[62] M. Hirai, S. Kumano, and N. Saito, Determination of polarized parton distribution functions with recent data on polarization asymmetries, Phys. Rev. D **74**, 014015 (2006).

[63] M. Hirai and S. Kumano (Asymmetry Analysis Collaboration), Determination of gluon polarization from deep inelastic scattering and collider data, Nucl. Phys. **B813**, 106 (2009).

[64] M. Glück, E. Reya, M. Stratmann, and W. Vogelsang, Models for the polarized parton distributions of the nucleon, Phys. Rev. D **63**, 094005 (2001).

[65] E. Leader, A. V. Sidorov, and D. B. Stamenov, A new evaluation of polarized parton densities in the nucleon, Eur. Phys. J. C **23**, 479 (2002).

[66] D. de Florian, R. Sassot, M. Stratmann, and W. Vogelsang, Global analysis of helicity parton densities and their uncertainties, Phys. Rev. Lett. **101**, 072001 (2008).

[67] D. de Florian, R. Sassot, M. Stratmann, and W. Vogelsang, Extraction of spin-dependent parton densities and their uncertainties, Phys. Rev. D **80**, 034030 (2009).

[68] J. Blümlein and S. Kurth, Harmonic sums and Mellin transforms up to two loop order, Phys. Rev. D **60**, 014018 (1999).

[69] J. Blümlein, A. De Freitas, W. L. van Neerven, and S. Klein, The longitudinal heavy quark structure function $F_L^{Q\bar{Q}}$ in the region $Q^2 \gg m^2$ at $O(\alpha_s^3)$, Nucl. Phys. **B755**, 272 (2006).

[70] S. Moch, J. A. M. Vermaseren, and A. Vogt, On γ_5 in higher-order QCD calculations and the NNLO evolution of the polarized valence distribution, Phys. Lett. B **748**, 432 (2015).

[71] J. Blümlein and N. Kochelev, On the twist-2 and twist-3 contributions to the spin dependent electroweak structure functions, Nucl. Phys. **B498**, 285 (1997).

[72] Y. Matiounine, J. Smith, and W. L. van Neerven, Two loop operator matrix elements calculated up to finite terms for polarized deep inelastic lepton—hadron scattering, Phys. Rev. D **58**, 076002 (1998).

[73] J. Blümlein, Analytic continuation of Mellin transforms up to two loop order, Comput. Phys. Commun. **133**, 76 (2000).

[74] J. Blümlein and M. Saragese (to be published).

[75] J. Blümlein, S. Riemersma, W. L. van Neerven, and A. Vogt, Theoretical uncertainties in the QCD evolution of structure functions and their impact on $\alpha_s(M_Z^2)$, Nucl. Phys. B, Proc. Suppl. **51**, 97 (1996).

[76] G. Rossi, Singularities in the perturbative QCD treatment of the photon structure functions, Phys. Lett. **130B**, 105 (1983).

[77] G. Rossi, X-space analysis for the photon structure functions in QCD, Phys. Rev. D **29**, 852 (1984).

[78] M. Glück, E. Reya, and A. Vogt, Parton structure of the photon beyond the leading order, Phys. Rev. D **45**, 3986 (1992).

[79] A. Vogt, Efficient evolution of unpolarized and polarized parton distributions with QCD-PEGASUS, Comput. Phys. Commun. **170**, 65 (2005).

[80] S. Alekhin, J. Blümlein, K. Daum, K. Lipka, and S. Moch, Precise charm-quark mass from deep-inelastic scattering, Phys. Lett. B **720**, 172 (2013).

[81] P. A. Zyla *et al.* (Particle Data Group), Review of particle physics, Prog. Theor. Exp. Phys. **2020**, 083C01 (2020).

[82] K. G. Chetyrkin, B. A. Kniehl, and M. Steinhauser, Strong coupling constant with flavor thresholds at four loops in the MS scheme, Phys. Rev. Lett. **79**, 2184 (1997).

[83] D. J. Gross and F. Wilczek, Ultraviolet behavior of nonAbelian gauge theories, Phys. Rev. Lett. **30**, 1343 (1973).

[84] H. D. Politzer, Reliable perturbative results for strong interactions, Phys. Rev. Lett. **30**, 1346 (1973).

[85] W. E. Caswell, Asymptotic behavior of nonAbelian gauge theories to two loop order, Phys. Rev. Lett. **33**, 244 (1974).

[86] D. R. T. Jones, Two loop diagrams in Yang-Mills theory, Nucl. Phys. **B75**, 531 (1974).

[87] O. V. Tarasov, A. A. Vladimirov, and A. Y. Zharkov, The Gell-Mann-low function of QCD in the three loop approximation, Phys. Lett. **93B**, 429 (1980).

[88] S. A. Larin and J. A. M. Vermaseren, The three loop QCD β function and anomalous dimensions, Phys. Lett. B **303**, 334 (1993).

[89] T. van Ritbergen, J. A. M. Vermaseren, and S. A. Larin, The four loop β function in quantum chromodynamics, Phys. Lett. B **400**, 379 (1997).

[90] M. Czakon, The four-loop QCD β-function and anomalous dimensions, Nucl. Phys. **B710**, 485 (2005).

[91] K. G. Chetyrkin, Four-loop renormalization of QCD: Full set of renormalization constants and anomalous dimensions, Nucl. Phys. **B710**, 499 (2005).

[92] P. A. Baikov, K. G. Chetyrkin, and J. H. Kühn, Five-loop running of the QCD coupling constant, Phys. Rev. Lett. **118**, 082002 (2017).

[93] F. Herzog, B. Ruijl, T. Ueda, J. A. M. Vermaseren, and A. Vogt, The five-loop β function of Yang-Mills theory with fermions, J. High Energy Phys. 02 (2017) 090.

[94] T. Luthe, A. Maier, P. Marquard, and Y. Schröder, The five-loop β function for a general gauge group and anomalous dimensions beyond Feynman gauge, J. High Energy Phys. 10 (2017) 166.

[95] D. Boer, M. Diehl, R. Milner, R. Venugopalan, W. Vogelsang, D. Kaplan, H. Montgomery, S. Vigdor, A. Accardi, E. C. Aschenauer *et al.*, Gluons and the quark sea at high energies: Distributions, polarization, tomography, arXiv:1108.1713.